Macromolecular Materials and Engineering
www.mme-journal.de

Honeycomb Surface with Shape Memory Behavior Fabricated via Breath Figure Process

Chien Hsin Wu, Chih Sheng Lu, Wei Lun Chen, Shih Huang Tung, and Ru Jong Jeng**

A bio-inspired honeycomb pattern that exhibits shape memory behavior is successfully fabricated via the breath figure process. By the surface modification along with a chemical crosslinking process to enhance the recoverability, this honeycomb-like structure with shape memory behavior is realized. The surface wettability is dependent on the surface topography controlled by the deformation of temporary shape (elliptical circle) and recovery of the permanent shape (round circle) at the microscopic scales without the need of micromolding or expensive lithography strategy. This approach opens a facile route to an efficient, inexpensive, and versatile method to prepare films with switchable wettability.

1. Introduction

Inspired by nature, the breath figure (BF) method is one of the most attractive self-assembly techniques for fabricating orderly packed pores with a hexagonal array due to its simplicity and versatility.[1–5] Traditional honeycomb films from the BF method exhibit circular pores on the surface because the honeycomb surfaces are created by water droplets as templates on a polymer solution under the condition of partial wetting.[6–8]

To go after special applications, several researchers deformed the microporous films via secondary processes to create unconventional honeycomb surfaces. Shimomura and co-workers[9] reported the mechanically stretchable deformation of honeycomb films to various geometric patterns from a polymer. The isotropic array of honeycomb surface was transformed into anisotropic alignment of micropores. This stretched microporous film as cell culture substrate can act as guidance to control the micropattern of cell growth. Furthermore, the same group[10] also demonstrated a shrinkable film by transferring the honeycomb film from glass substrate onto a shrinkable polymer. After repeated cycles of thermal shrinking, the sizes of the pits on the surface were reduced from several micrometers to hundreds of nanometers. In addition, Li et al.[11] developed a noncontact photomanipulation strategy for tuning the shape of honeycomb pores based on an azobenzene containing polymer. Under the irradiation of linearly polarized light, round pores of honeycomb were converted into rectangular, rhombic, and parallelogram shapes. By means of a secondary irradiation by rotating the sample 90°, the deformed pores almost recovered to the original as-prepared film. These above-mentioned studies mainly focus on the deformation of honeycomb pores, whereas our current research emphasizes on the shape memory effect of honeycomb structures, i.e., the shape fixity and recovery.

Shape memory polymers (SMPs) are a class of stimuli-response materials.[12] Microstructures fabricated on an SMP may create a reversibly tunable surface. Usually, the shape memory effect was programmed by thermal phase transitions including glass transition (T_g), melting temperature (T_m), or liquid crystal temperature (T_c).[13–15] By changing shape in the low modulus state above the phase transition temperature, SMPs are capable of deforming a permanent shape to a temporary shape. The temporary shape would be preserved in the high modulus state below the phase transition temperature unless the temperature rises up above the phase transition. Therefore, any microstructural changes may translate into the deformation and recovery occurs at macroscopic scale of SMPs. One of the excellent examples is the use of micropillar fabricated via a lithography method on an SMP surface demonstrated by Yang and co-worker.[16] The surface exhibited distinct wettability according to the deformed or original/recovered SMP pillar array. These micropillar SMPs exhibit potential for the applications of water collection or optical devices. Nevertheless, most of the microfabrication methods on SMPs are based on expensive lithography[16–20] or complicated micromolding[21–24] strategy. Therefore, it is sensible to probe a microstructure with switchable wettability produced without the need of resorting to micromolding or expensive lithography strategy. Our approach is to fabricate a microstructure with shape memory behavior and subsequently to demonstrate the reversible wettability of SMP films, depending on the deformed or original/recovered honeycomb-like structures.

Poly(urea/malonamide) dendrons have been utilized for fabricating honeycomb-like structures through the BF process.[25–29] The hexagonal array of micropores could be achieved by either grafting dendrons onto the side groups of polymers or blending dendrons with polymers. In addition, we have reported that the polyurethanes (PUs) with poly(urea/malonamide) dendrons as chain extenders also exhibited shape memory behavior.[30,31] Therefore, it is possible to fabricate honeycomb-like films with

Dr. C. H. Wu, C. S. Lu, W. L. Chen, Prof. S. H. Tung, Prof. R. J. Jeng
Institute of Polymer Science and Engineering
National Taiwan University
No. 1, Sec. 4, Roosevelt Rd., Taipei 10617, Taiwan (R.O.C.)
E-mail: shtung@ntu.edu.tw; rujong@ntu.edu.tw
The ORCID identification number(s) for the author(s) of this article can be found under https://doi.org/10.1002/mame.201700433.

DOI: 10.1002/mame.201700433

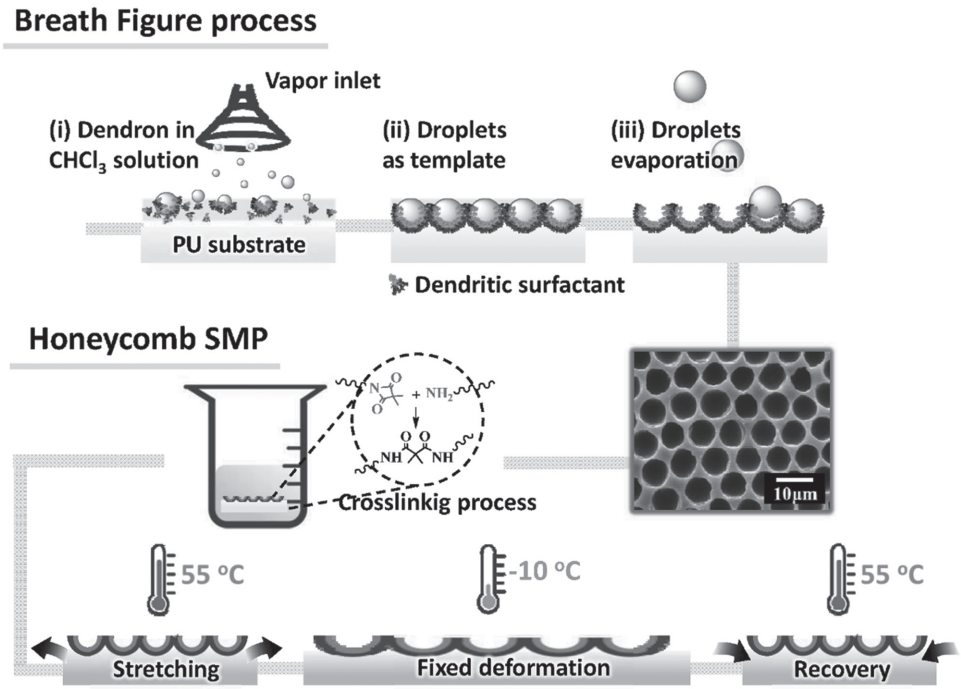

Scheme 1. Preparation of honeycomb-like surface with shape memory behavior.

shape memory effect based on the PUs we have developed. In fact, honeycomb-like films could be achieved through the BF process using the above-mentioned shape memory PUs. However, the direct investigation of the shape memory behavior is not possible. This is because the thickness of the honeycomb-like films (with high porosity) from the BF process is usually less than several micrometers,[32–34] unable to provide a sufficient mechanical strength for shape fixity and shape recovery.

In this work, we adopt a different approach to prepare honeycomb-like structure on PU substrates with shape memory effect as shown in **Scheme 1**. This strategy is aiming at growing the honeycomb-like surface of thick PU substrates without succumbing to the thickness issue for the traditional BF method. Chemically cross-linkable PUs with active azetidine-2,4-diones as side groups (S45, where 45 is the PU with 45 wt% hard segment (HS) content; Figure S1 and Table S1, Supporting Information) were utilized as the substrate materials. The azetidine-2,4-dione-containing poly(urea/malonamide) dendron was utilized as surfactant to form a honeycomb-like structure on the PU substrates via the BF process (Figure S2, Supporting Information).[25] It is important to note that the azetidine-2,4-dione functional group is capable of reacting with primary amine containing reagents to obtain malonamide linkage under mild conditions.[35]

2. Results and Discussion

Honeycomb-like surfaces were fabricated via the BF process under the assistance of dendrons. First, a solution of poly(urea/malonamide) dendron dissolved in chloroform was drop-cast on the surface of the PU films under a humid condition. When the water vapor condensed on the surface of dendrons/chloroform solution, the water droplets were stabilized by amphiphilic poly(urea/malonamides) to circumvent aggregation. Subsequently, the evaporation of chloroform facilitated the condensation of water vapor as the condensed water droplets floating on the solution surface self-organized into close-packed hexagonal arrays. Upon complete evaporation of the solvent and water, a porous honeycomb-like structure with azetidine-2,4-dione functional groups was ready for further chemical crosslinking reactions as shown in Scheme 1.

The honeycomb-like surface was treated with 1,6-hexanediamine (HDA) in aqueous solution for 1 h to proceed the crosslinking process. It is noted that water is a poor solvent to Pus; consequently, the concentration of HDA is relatively low in bulk polymer to prevent the formation of one end HDA. This HDA diffusion in bulk S45 was controlled by the HDA aqueous solutions in different concentrations, and the residual HDA was removed by deionic (DI) water. After the reaction of aztidine-2,4-dione functional groups with HDA, the crosslinked honeycomb-like surface was achieved without the disruption of morphology.

The ring opening reaction was monitored by attenuated total reflection-infrared (ATR-IR) spectroscopy. In order to have a better insight into the crosslinking process, the experiments were conducted on the smooth films instead of porous ones because the honeycomb-like structure may interfere with the IR signal. The crosslinked S45 samples were prepared by the reaction with HDA in aqueous solution at concentrations of 0.2 M, 0.5 M, and 1.0 M for 1 h to obtain C45-1, C45-2, and C45-3, respectively (Table S1, Supporting Information). The ATR-IR spectra are shown in **Figure 1**a. S45 comprising aztidine-2,4-diones exhibited adsorption peaks at 1855 cm^{-1} (C=O asymmetric stretching) and 1726 cm^{-1} (C=O symmetric stretching).

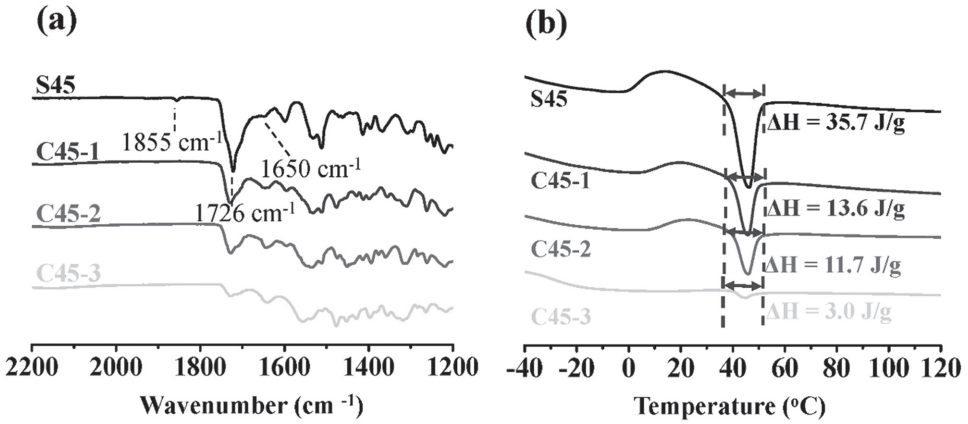

Figure 1. Chemical crosslinking process investigated by a) ATR-IR spectra, and b) DSC thermograms for neat and cross-linked PUs.

As the crosslinking reaction proceeded, the intensities of these two peaks decreased, along with the emergence of an absorption peak at 1650 cm^{-1} due to the formation of malonamide linkage. Based on the above, the degree of crosslinking reaction increased with increasing HDA concentration.

It is well known that the soft segments (SS) and HS on PUs are usually immiscible and tend to phase separate into soft and hard domains. The molecular interactions and the crystallinity in each domain greatly influence the properties of PUs.[36] To obtain this information, the thermal properties of the PUs were monitored by differential scanning calorimeter (DSC) as shown in Figure 1b. During the second heating scan, S45 exhibited an endothermic peak at 43 °C, which is attributed to the melting transition of crystalline polycaprolactone in soft domains. The melting enthalpy (ΔH) is highly dependent on the degree of chemical crosslinking reaction. For S45 (ΔH = 35.7 J g^{-1}), a decreased melting enthalpy with increased degree of crosslinking reaction was observed, C45-1 (ΔH = 13.6 J g^{-1}), C45-2 (ΔH = 11.7 J g^{-1}), and C45-3 (ΔH = 3.5 J g^{-1}), because the crosslinking restricts the SS mobility as well as prevents the SS from close packing.

Figure 2a shows the thermal–mechanical properties for the PU samples with various degrees of chemical crosslinking reaction. At temperatures higher than 10 °C, the sharp decrease of the storage modulus (E') was mainly attributed to the melting of SS as observed in the DSC thermograms (Figure 2a). No rubber plateau could be found for S45 after the melting of soft domains, indicating that the content of HS in S45 is insufficient to form stable hard domains that can serve as physical crosslinks. In contrast, C45-1, C45-2, and C45-3 showed clear rubber plateaus, confirming the chemical crosslinking in these samples. As expected, E' of the rubber plateau increased with increasing degree of chemical crosslinking.

With a rather steep drop of E' upon melting in soft domains and a broad rubbery plateau, C45-1 and C45-2 are good candidates for shape memory applications.[15] The shape memory properties of samples were tested using dynamic mechanical analyzer (DMA). At first, samples were stretched to 100% deformation in rubber state at 55 °C (step 1) where the chemical crosslinks in hard domains could suppress a permanent deformation. Subsequently, the sample deformation was fixed by cooling the sample to −10 °C (step 2), below the onset temperature of SS melting, where the molecular motion was greatly restricted to prevent the chains from a large-scale relaxation. Therefore, their temporary deformed shape could be effectively maintained after the removal of an external force (step 3). The ratio of shape fixity (R_f) was calculated by Equation (1), where ε_m and ε_u are the strains in step 1 and step 3, respectively. This temporary shape was maintained until the

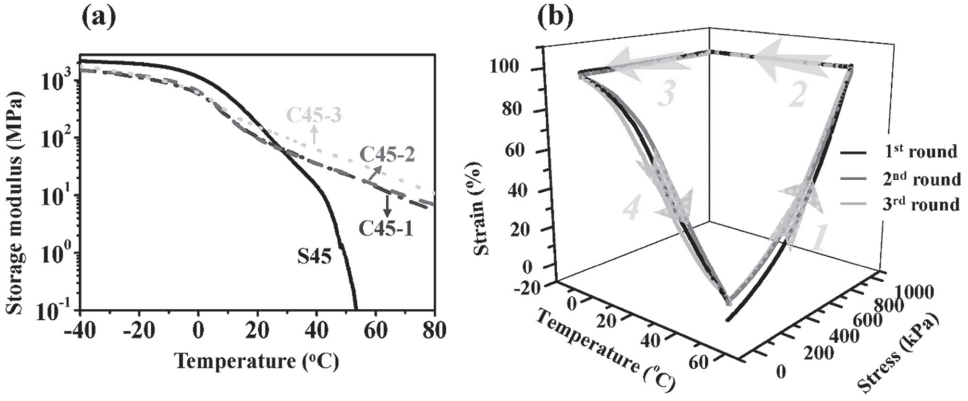

Figure 2. a) DMA thermograms for neat and cross-linked PUs, and b) 3D plot of the shape memory cycle for C45-1: deformed at 55 °C (step 1), cooled to −10 °C (step 2), unloaded stress at −10 °C (step 3), and recovered for one cycle (step 4).

samples were heated to 55 °C in the final step to end a cycle of shape memory process (step 4). The polymer chains at this temperature regain the mobility and tend to recover their original shape because of the rubber elasticity provided by the chemical crosslinks. The ability of sample recovery could be quantified through the calculation of shape recovery (R_r) according to Equation (2), where ε_p is the strain of the permanent deformation. This cycle was repeated for three times to estimate the reproducibility of shape memory behavior

$$\text{Shape fixity, } R_f\ (\%) = \varepsilon_u/\varepsilon_m \times 100\% \quad (1)$$

$$\text{Shape recovery, } R_r\ (\%) = \left(\varepsilon_m - \varepsilon_p\right)/\varepsilon_m \times 100\% \quad (2)$$

After three cycles of the shape memory test, C45-1 exhibited the best R_f and R_r among all the PUs as well as good reproducibility of shape memory performance (Figure 2b and Table S2, Supporting Information). This result indicates that the fraction of soft segments and the degree of chemical crosslinking in C45-1 are optimal to simultaneously provide stretchability and recoverability while the crystallinity of soft domains is sufficient to effectively fix the deformed shape.

Having known that C45-1 shows the best shape memory property, the honeycomb-like structure was formed through the BF process on the S45 surface and then the sample was crosslinked in the 0.2 M HDA aqueous solution to obtain C45-1 with both honeycomb-like surface and shape memory behavior. The scanning electron microscope (SEM) images of the smooth S45 and honeycomb-like C45-1 films are shown in **Figure 3**. The morphology of honeycomb-like structure remained virtually intact after the crosslinking process (Figure 3b). Subsequently, the sample was stretched in the axial direction to 100% at 55 °C and then frozen at −10 °C where the fixed elliptical pores were observed as shown in Figure 3c. After heating the sample at 55 °C for 30s, the elliptical pores recovered their original round shape as shown in Figure 3d. This deformed surface was able to return to its original shape after three rounds of stretching and recovery process, indicating the success of fabricating shape memory honeycomb-like structure.

The water wettability on the honeycomb-like surface could be manipulated by the shape deformation and recovery. As shown in Figure 3a–d, the honeycomb-like surface exhibited a higher contact angle (94.1°) than the smooth PU surface (70.5°) due to the increased surface roughness. The contact angle of the deformed honeycomb-like structure was further increased to 121.3° due to the presence of the increased pore sizes when the sample was stretched (see Casse and Baxter's law).[37] After recovering from the deformed state, the contact angle was back to 97.8°, close to the original value. The result shows that a reversible wettability can be achieved through the combination of BF process and shape memory substrates, i.e., honeycomb-like structure with shape memory effect. After 100% uniaxial strain, the pores (diameter 5.7 μm) went from circle to ellipse (major axis 8.8 μm; minor axis 4.7 μm; Figure 3e). The observed uniaxial local strain was about 54%. Upon recovery, the pore sizes recovered to a diameter of 6.2 μm with about 9% residual strain. Upon deformation, the rim widths in the major and minor axes increased significantly due to the formation of extended elliptical pores (Figure 3f). After recovery, the rim width decreased to 1.7 μm, similar to that of the pristine sample.

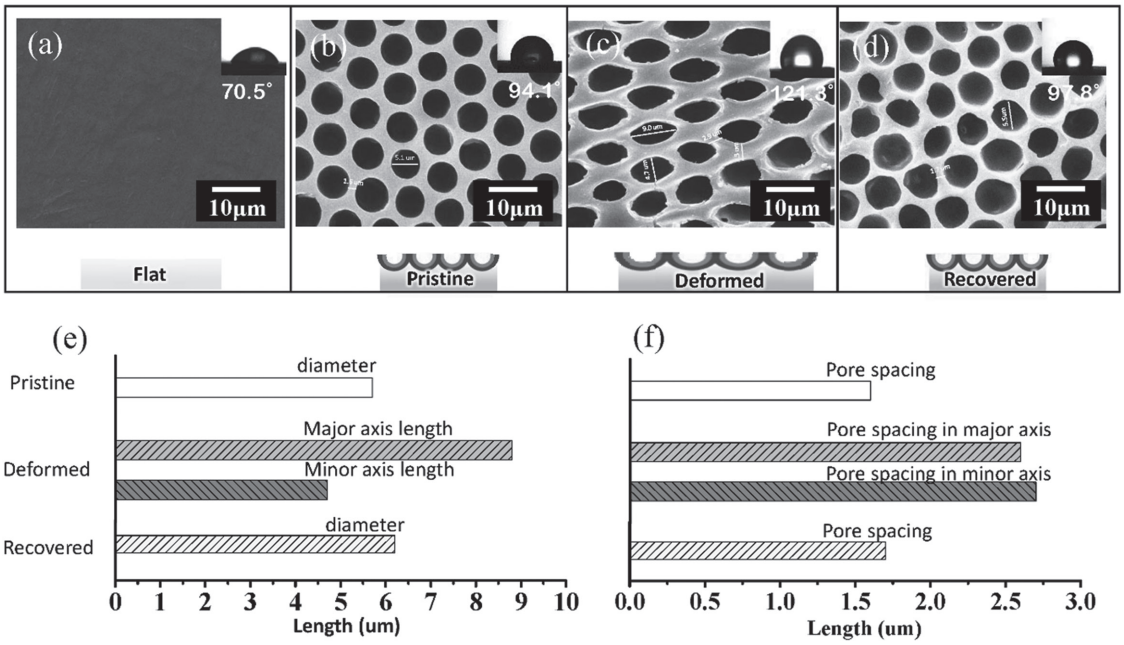

Figure 3. SEM images of flat and honeycomb-like films, average pore sizes, and rim widths. a) S45 flat substrate; b) honeycomb surface on the SMP substrate through BF process following the crosslinking procedure; c) the deformed honeycomb surface by axial stretching at temperatures above switching phase (55 °C), followed by the cooling process to −10 °C; d) the deformed surface recovered to its original shape by heating at 55 °C, histogram for average e) pore sizes, and f) rim widths between pores (contact angles corresponding to original and deformed morphologies are shown on the up right).

3. Conclusions

In summary, a simple method to fabricate a microstructure with reversible wettability was achieved on the surface of a shape memory polymer substrate. The honeycomb-like surface was prepared through a bio-inspired self-assembly, i.e., the breath figure method, without the need of micromolding or expensive lithography strategy. By the surface modification along with a chemical crosslinking process to enhance the recoverability, this honeycomb-like structure with shape memory behavior was realized. This approach opens a facile route to an efficient, inexpensive, and versatile method to prepare films with switchable wettability.

Supporting Information

Supporting Information is available from the Wiley Online Library or from the author.

Acknowledgements

This work was supported by the Ministry of Science and Technology of Taiwan.

Conflict of Interest

The authors declare no conflict of interest.

Keywords

breath figure, honeycomb-like film, polyurethane, shape memory

Received: August 31, 2017
Revised: October 16, 2017
Published online: December 4, 2017

[1] U. H. F. Bunz, *Adv. Mater.* **2006**, *18*, 973.
[2] C.-Y. Ma, Y.-W. Zhong, J. Li, C.-K. Chen, J.-L. Gong, S.-Y. Xie, L. Li, Z. Ma, *Chem. Mater.* **2010**, *22*, 2367.
[3] M. Hernandez-Guerrero, M. H. Stenzel, *Polym. Chem.* **2012**, *3*, 563.
[4] A. Zhang, H. Bai, L. Li, *Chem. Rev.* **2015**, *115*, 9801.
[5] A. Bertrand, A. Bousquet, C. Lartigau-Dagron, L. Billon, *Chem. Commun.* **2016**, *52*, 9562.
[6] P. Escalé, L. Rubatat, L. Billon, M. Save, *Eur. Polym. J.* **2012**, *48*, 1001.
[7] L.-S. Wan, L.-W. Zhu, Y. Ou, Z.-K. Xu, *Chem. Commun.* **2014**, *50*, 4024.
[8] G. Widawski, M. Rawiso, B. Francois, *Nature* **1994**, *369*, 387.
[9] T. Nishikawa, M. Nonomura, K. Arai, J. Hayashi, T. Sawadaishi, Y. Nishiura, M. Hara, M. Shimomura, *Langmuir* **2003**, *19*, 6193.
[10] H. Yabu, R. Jia, Y. Matsuo, K. Ijiro, S.-A. Yamamoto, F. Nishino, T. Takaki, M. Kuwahara, M. Shimomura, *Adv. Mater.* **2008**, *20*, 4200.
[11] W. Wang, C. Du, X. Wang, X. He, J. Lin, L. Li, S. Lin, *Angew. Chem., Int. Ed.* **2014**, *53*, 12116.
[12] Q. Zhao, H. J. Qi, T. Xie, *Prog. Polym. Sci.* **2015**, *49–50*, 79.
[13] T. Hisaaki, H. Hisashi, Y. Etsuko, H. Shunichi, *Smart Mater. Struct.* **1996**, *5*, 483.
[14] A. Lendlein, S. Kelch, *Angew. Chem., Int. Ed.* **2002**, *41*, 2034.
[15] C. Liu, H. Qin, P. T. Mather, *J. Mater. Chem.* **2007**, *17*, 1543.
[16] C.-M. Chen, S. Yang, *Adv. Mater.* **2014**, *26*, 1283.
[17] B. A. Nelson, W. P. King, K. Gall, *Appl. Phys. Lett.* **2005**, *86*, 103108.
[18] S. Reddy, E. Arzt, A. del Campo, *Adv. Mater.* **2007**, *19*, 3833.
[19] Z. Wang, C. Hansen, Q. Ge, S. H. Maruf, D. U. Ahn, H. J. Qi, Y. Ding, *Adv. Mater.* **2011**, *23*, 3669.
[20] J. Li, J. Shim, J. Deng, J. T. B. Overvelde, X. Zhu, K. Bertoldi, S. Yang, *Soft Matter* **2012**, *8*, 10322.
[21] C.-M. Chen, C.-L. Chiang, C.-L. Lai, T. Xie, S. Yang, *Adv. Funct. Mater.* **2013**, *23*, 3813.
[22] E. Lee, M. Zhang, Y. Cho, Y. Cui, J. Van der Spiegel, N. Engheta, S. Yang, *Adv. Mater.* **2014**, *26*, 4127.
[23] S. Kim, M. Sitti, T. Xie, X. Xiao, *Soft Matter* **2009**, *5*, 3689.
[24] C.-M. Chen, C.-L. Chiang, S. Yang, *Langmuir* **2015**, *31*, 9523.
[25] C.-H. Wu, W.-H. Ting, Y.-W. Lai, S. A. Dai, W.-C. Su, S.-H. Tung, R.-J. Jeng, *RSC Adv.* **2016**, *6*, 91981.
[26] Y. A. Su, W. F. Chen, T. Y. Juang, W. H. Ting, T. Y. Liu, C. F. Hsieh, S. H. A. Dai, R. J. Jeng, *Polymer* **2014**, *55*, 1481.
[27] C. C. Chang, T. Y. Juang, W. H. Ting, M. S. Lin, C. M. Yeh, S. A. Dai, S. Y. Suen, Y. L. Liu, R. J. Jeng, *Mater. Chem. Phys.* **2011**, *128*, 157.
[28] W. H. Ting, C. C. Chen, S. A. Dai, S. Y. Suen, I. K. Yang, Y. L. Liu, F. M. C. Chen, R. J. Jeng, *J. Mater. Chem.* **2009**, *19*, 4819.
[29] C.-Y. Chiang, T.-Y. Liu, Y.-A. Su, C.-H. Wu, Y.-W. Cheng, H.-W. Cheng, R.-J. Jeng, *Polymers* **2017**, *9*, 93.
[30] C.-H. Wu, S.-M. Shau, S.-C. Liu, S. A. Dai, S.-C. Chen, R.-H. Lee, C.-F. Hsieh, R.-J. Jeng, *RSC Adv.* **2015**, *5*, 16897.
[31] C. C. Tsai, C. C. Chang, C. S. Yu, S. A. Dai, T. M. Wu, W. C. Su, C. N. Chen, F. M. C. Chen, R. J. Jeng, *J. Mater. Chem.* **2009**, *19*, 8484.
[32] T. Hayakawa, S. Horiuchi, *Angew. Chem., Int. Ed.* **2003**, *42*, 2285.
[33] A. Bolognesi, C. Mercogliano, S. Yunus, M. Civardi, D. Comoretto, A. Turturro, *Langmuir* **2005**, *21*, 3480.
[34] A. Bolognesi, F. Galeotti, U. Giovanella, F. Bertini, S. Yunus, *Langmuir* **2009**, *25*, 5333.
[35] C.-P. Chen, S. A. Dai, H.-L. Chang, W.-C. Su, R.-J. Jeng, *J. Polym. Sci., Part A: Polym. Chem.* **2005**, *43*, 682.
[36] R. W. Seymour, S. L. Cooper, *Macromolecules* **1973**, *6*, 48.
[37] E. Min, K. H. Wong, M. H. Stenzel, *Adv. Mater.* **2008**, *20*, 3550.

